Xanthatin Selectively Targets Retinoblastoma by Inhibiting the PLK1-Mediated Cell Cycle

Jie Yang,[1,2,*] Yongyun Li,[1,2,*] Chunyan Zong,[1,2] Qianqian Zhang,[3] Shengfang Ge,[1,2] Lei Ma,[4] Jiayan Fan,[1,2,#] Jianming Zhang,[3,#] and Renbing Jia[1,2,#]

[1]Department of Ophthalmology, Ninth People's Hospital, Shanghai Jiao Tong University School of Medicine, Shanghai, China
[2]Shanghai Key Laboratory of Orbital Diseases and Ocular Oncology, Shanghai, China
[3]National Research Center for Translational Medicine, State Key Laboratory of Medical Genomics, Rui-Jin Hospital, Shanghai Jiao Tong University School of Medicine, Shanghai, China
[4]Shanghai Key Laboratory of New Drug Design, School of Pharmacy, East China University of Science and Technology, Shanghai, China

Correspondence: Renbing Jia, Department of Ophthalmology, Ninth People's Hospital, Shanghai Jiao Tong University School of Medicine, No. 639, Zhizaoju Road, Huangpu District, Shanghai 200001, China; renbingjia@sjtu.edu.cn.
Jiayan Fan, Department of Ophthalmology, Ninth People's Hospital, Shanghai Jiao Tong University School of Medicine, No. 12, Lane 833, Zhizaoju Road, Shanghai 200001, China; fanjiayan1118@126.com.
Jianming Zhang, National Research Center for Translational Medicine, State Key Laboratory of Medical Genomics, Rui-Jin Hospital, Shanghai Jiao Tong University School of Medicine, Shanghai 20025, China; jzuc@shsmu.edu.cn.

JY and YL contributed equally to this work.
JF, JZ and RJ are co-corresponding authors of this work.

Received: April 6, 2021
Accepted: November 12, 2021
Published: December 13, 2021

Citation: Yang J, Li Y, Zong C, et al. Xanthatin selectively targets retinoblastoma by inhibiting the PLK1-mediated cell cycle. *Invest Ophthalmol Vis Sci.* 2021;62(15):11. https://doi.org/10.1167/iovs.62.15.11

Purpose. Retinoblastoma is the most common primary intraocular malignant tumor in children. Although intra-arterial chemotherapy and conventional chemotherapy have become promising therapeutic approaches for advanced intraocular retinoblastoma, the side effects threaten health and are unavoidable, making the development of targeted therapy an urgent need. Therefore, we intended to find a potential drug for human retinoblastoma by screening an in-house compound library that included 89 purified and well-characterized natural products.

Methods. We screened a panel of 89 natural products in retinoblastoma cell lines to find the inhibitor. The inhibition of the identified inhibitor xanthatin on cell growth was detected through half-maximal inhibitory concentration (IC_{50}), flow cytometry assay, and zebrafish model system. RNA-seq further selected the target gene PLK1.

Results. We reported the discovery of xanthatin as an effective inhibitor of retinoblastoma. Mechanistically, xanthatin selectively inhibited the proliferation of retinoblastoma cells by inducing cell cycle arrest and promoting apoptosis. Interestingly, xanthatin targeted PLK1-mediated cell cycle progression. The efficacy of xanthatin was further confirmed in zebrafish models.

Conclusions. Collectively, our data suggested that xanthatin significantly inhibited tumor growth in vitro and in vivo, and xanthatin could be a potential drug treatment for retinoblastoma.

Keywords: Xanthatin, retinoblastoma, cell cycle, PLK1

Retinoblastoma is the most common and aggressive primary intraocular malignant tumor in children, and the age of onset is under 3 years old in most patients.[1,2] In developing countries, delayed diagnosis leads to sequelae and high patient mortality.[3–6] At present, enucleation is less frequently used in developed countries. According to the size, location, and scope of the tumor, intravenous and ophthalmic arterial interventional chemotherapy and local treatment (laser, transpupillary thermotherapy, cryotherapy, and radionuclide therapy) are used to preserve the eyeballs and even vision. The carboplatin, etoposide, and vincristine (CEV) regimen is a common chemotherapeutic approach for the treatment of middle- or late-stage retinoblastoma.[7,8] When the risk of tumor metastasis is high and the application of conventional chemotherapy is not feasible, enucleation must be considered.

Copyright 2021 The Authors

This work is licensed under a Creative Commons Attribution-NonCommercial-NoDerivatives 4.0 International License.

Downloaded from hwmaint.iovs.org on 04/25/2024

Intra-arterial chemotherapy (IAC), also known as superselective ophthalmic artery chemotherapy, has become a main technology for the treatment of advanced intraocular retinoblastoma to protect children's eyeballs.[9,10] However, melphalan and topotecan often exert strong cytotoxic effects. In addition, drug resistance and the side effects of chemotherapy increase in response to prolonged treatment.[11,12] In severe cases, enucleation and even removal of the orbital content must be performed. These consequences could seriously impair children's appearance and quality of life. Retinoblastoma may even lead to death from systemic metastasis as the disease progresses.[13] Therefore, there is still opportunities for improving the treatment of retinoblastoma to meet clinical needs.

Traditional Chinese medicine (TCM) has been practiced for thousands of years in China and East Asia. In some areas, it is a predominant medical practice to prescribe Chinese herbal medicine due to its efficient curative power and mild side effects, as well as economic reasons and religious beliefs.[14,15] A large number of natural drugs have been used in clinical applications, which are derived originally from natural sources in human history. For example, the arsenic trioxide (As2O3) therapy used for acute promyelocytic leukemia, homoharringtonine for chronic myeloid leukemia, the antibiotic penicillin for bacterial infection, the aspirin for secondary prevention of cardiovascular diseases, and artemisinin for combating malaria.[16,17] The components of Chinese herbal medicine are complex mixtures and often have multiple cellular targets. In many cases, it is difficult to understand the main active ingredients of herbal medicine or elucidate the molecular mechanism of action. This situation often hinders the further development and optimization of Chinese herbal medicine in vivo. Nevertheless, we aimed to investigate the utility of natural compounds in treating retinoblastoma with the hope of providing potential systemic therapies.

Here, we screened a panel of 89 natural products in retinoblastoma cell lines. This in-house compound library is composed of single components purified from Chinese herbal medicine. We aimed to determine whether Chinese herbal medicines currently used in the clinic might have potential activity against retinoblastoma. Xanthatin has been identified as an effective inhibitor of retinoblastoma. Further studies showed that xanthatin exerted its pharmacological effects by inhibiting the PLK1-mediated G2/M pathway and inducing apoptotic death of retinoblastoma cells. Collectively, xanthatin showed the potential to be developed as a novel therapeutic agent for patients with retinoblastoma.

Materials and Methods

Cell Culture

The retinoblastoma cell line Y79 was obtained from ATCC, and the cell line WERI-Rb1 was obtained from the Cell Bank/Stem Cell Bank (Chinese Academy of Sciences). The uveal melanoma (UM) cell lines OMM2.3 and MEL290 were kindly provided by Professor Martine J. Jager (Leiden University Medical Center, Leiden, The Netherlands). The adult retinal pigment epithelium cell line ARPE-19 was obtained from the Cell Bank/Stem Cell Bank (Chinese Academy of Sciences). The cells were cultured in RPMI-1640 medium (Gibco, USA). All the media were supplemented with 10% fetal bovine serum (Gibco, USA), 1% penicillin and streptomycin, and the cells were incubated at 37°C with 5% CO_2.

Drug Screening

To identify retinoblastoma-specific compounds, the retinoblastoma cell lines Y79 and WERI-Rb1 and the UM cell lines OMM2.3 and MEL290 were subjected to viability screening after exposure to an in-house compound library that included 89 purified and well-characterized natural products (Supplementary Table S1). Retinoblastoma cells were seeded at 3000 cells/well and UM cells were seeded at 800 cells/well in a 384–well plate using automated plate filler. Subsequently, a 2-µM concentration of each drug was added to the plate via pin transfer, and the plates were incubated for an additional 72 hours at 37°C. The pharmacological efficacy of the compounds was measured via cell viability using a CellTiter-Glo Luminescence assay (Promega) and an EnVision plate reader (PerkinElmer).

Cell Viability

Based on the results of the initial drug screen, two retinoblastoma cell lines (Y79 and WERI-Rb1) and two UM cell lines (OMM2.3 and MEL290) were selected for additional analysis of the drug xanthatin. The cells were seeded at 3000 cells/well in 96–well plates and subjected to 10 doses of xanthatin in 3 biological replicates. Cell viability was measured after incubation with the drugs for 72 hours at 37°C using a CCK-8 assay (Dojindo). An equivalent volume of DMSO was used as a control, and the results were normalized to the DMSO control. The half maximal inhibitory concentration (IC_{50}) values were calculated using GraphPad Prism software (version 7.0), and the comparison of IC_{50} values between the retinoblastoma and UM cell lines was performed by using unpaired *t*-tests.

Analysis of In Vivo Toxicity

To test compound toxicity, six zebrafish embryos (3 days post fertilization [dpf]) per well were placed into a 24-well plate containing 1 mL egg water, in which the compound was diluted at different concentrations. The embryos were incubated at 28°C. The drug-containing medium was refreshed every 2 days, and survival was evaluated up to 8 dpf. If the survival rate of the zebrafish embryos was higher than 80%, the compound was considered nontoxic.[18] To analyze the treatment effect, a dose of 300 Y79-mCherry cells was implanted in the 2-dpf yolk sac. At 1 day post injection (dpi), treatment of the implanted embryos was initiated with 5 µM xanthatin. Embryos were fixed with 4% paraformaldehyde (PFA) at 6 dpi.[19]

Apoptosis Assay

Annexin V-FITC/propidium iodide (PI) double staining was used to detect apoptosis by flow cytometry. Y79 transfected of PLK1 siRNA negative control siRNA for 48 hours and Y79 cells preincubated with xanthatin (0, 0.5, 1, and 2 µM) for 24 hours were collected by centrifugation, washed with PBS, and then stained with 0.3% Annexin V-FITC in binding buffer for 15 minutes at room temperature in the dark. After centrifugation and resuspension in 1× binding buffer, PI was added to the cells before flow cytometry analysis (Beckman CytoFLEX flow cytometer). The software CytExpert was used for data analysis.

Investigative Ophthalmology & Visual Science

Downloaded from hwmaint.iovs.org on 04/25/2024

Cell Cycle Assay

Y79 cells were treated with xanthatin (0, 0.5, 1, and 2 μM) for 24 hours, washed with PBS, and fixed with 66% ethanol overnight. The cells were washed with PBS and pelleted by centrifugation. Subsequently, the pellets were resuspended in PBS and stained with PI (50 μg/mL) and RNase (2.5 μg/mL) for 30 minutes at room temperature. The DNA content was analyzed by flow cytometry (Beckman CytoFLEX flow cytometer). The software CytExpert was used for data analysis.

Total RNA Sequencing

Total RNA from the Y79 and WERI-Rb1 cells treated with xanthatin (0 and 1 μM) for 24 hours was extracted with Trizol (Invitrogen) and assessed with Agilent 2100 BioAnalyzer (Agilent Technologies, Santa Clara, CA, USA) and Qubit Fluorometer (Invitrogen). Total RNA samples that met the following requirements were used in subsequent experiments: RNA integrity number (RIN) >7.0 and a 28S:18S ratio >1.8.RNA-seq libraries were generated and sequenced by CapitalBio Technology (Beijing, China). The triplicate samples of all assays were constructed in an independent library, and did the following sequencing and analysis. The NEB Next Ultra RNA Library Prep Kit for Illumina (NEB) was used to construct the libraries for sequencing. The NEB Next Poly(A) mRNA Magnetic Isolation Module (NEB) kit was used to enrich the poly(A) tailed mRNA molecules from 1 μg total RNA. The mRNA was fragmented into ~200 base pair pieces. The first-strand cDNA was synthesized from the mRNA fragments reverse transcriptase and random hexamer primers, and then the second-strand cDNA was synthesized using DNA polymerase I and RNaseH. The end of the cDNA fragment was subjected to an end repair process that included the addition of a single "A" base, followed by ligation of the adapters. Products were purified and enriched by polymerase chain reaction (PCR) to amplify the library DNA. The final libraries were quantified using KAPA Library Quantification kit (KAPA Biosystems, South Africa) and an Agilent 2100 Bioanalyzer. After quantitative reverse transcription-polymerase chain reaction (RT-qPCR) validation, libraries were subjected to paired-end sequencing with pair end 150-base pair reading length on an Illumina NovaSeq sequencer (Illumina).

RNA-seq: Data Analysis

The genome of human genome version of hg38 was used as the reference. The sequencing qualities were assessed with FastQC (version 0.11.5) and then low quality data were filtered using NGSQC (version 2.3.3).[20] The clean reads were then aligned to the reference genome using HISAT2 (version 2.1.0) with default parameters. The processed reads from each sample were aligned using HISAT2 against the reference genome. The gene expression analyses were performed with StringTie (version 1.3.3b).[21] DESeq (version 1.28.0)[22] was used to analyze the DEGs between samples. Thousands of independent statistical hypothesis testing was conducted on DEGs, separately. Then a P value was obtained, which was corrected by the false discovery rate (FDR) method. In addition, the corrected P value (q-value) was calculated by correcting using the Benjamini-Hochberg (BH) method. The P value or q-value were used to conduct significance analysis. Parameters for classifying significantly DEGs are ≥2-fold differences (|log2FC|≥1, FC: the fold change of expressions) in the transcript abundance and $P < 0.05$.

The annotation of the DEGs were performed based on the information obtained from the databases of ENSEMBL, National Center for Biotechnology Information (NCBI), Uniprot, Gene Ontology (GO), and Kyoto Encyclopedia of Genes and Genomes (KEGG).

RNA Extraction and Real-Time PCR Analysis

Total RNA was extracted using TRI-Reagent (Invitrogen, USA), and cDNA was synthesized using the PrimeScript RT reagent kit according to the manufacturer's instructions (Takara, Japan). Real-time PCR was performed using primers specific for PLK1, CCNB1, CDK1, UBE2C, and CENPA (Table). The relative expression of individual transcripts was normalized to GAPDH. The fold change of target mRNA expression was calculated based on the threshold cycle (Ct), where △Ct = Ct target - Ct18S and △ (△Ct) = △Ct Control - △Ct Indicated condition.

Western Blot Analysis

The antibodies used in Western blot analysis were PLK1 (CST, 4513T, 1:1000), CCNB1 (CST, 4138T, 1:1000), CDK1 (CST, 9116T, 1:1000), UBE2C (Abcam, ab252940, 1:1000), CENPA (CST, 2186T, 1:1000), and GAPDH (Bioworld, MB001, 1:5000). The immunoblots were visualized with the Odyssey infrared imaging system (LI-COR).

siRNA Assay

The sequences of two siRNA used to target PLK1 were listed as follows:

siPLK1-2: 5′- CGAUACUACCUACGGCAAA- 3′,
siPLK1-3: 5′- CGAGGUGCUGAGCAAGAAA- 3′.

Cells were incubated in Opti-MEM I Reduced Serum Medium (Gibco, USA) containing 50 nM siRNA and Lipofectamine 2000 (Invitrogen) at 37°C. Six hours after transfection, the medium was exchanged for RPMI-1640 medium supplemented with 10% fetal bovine serum (FBS), and the cells were maintained at 37°C for 48 hours.

CCK8 Assay

To determine cell viability, cells were seeded in 96-well plates at a density of 3000 cells per well. After incubation with 10 μL CCK-8 reagent (Dojindo Laboratories, Japan) per well, the absorbance was measured at a wavelength of 450 nm at the indicated time points. The data were recorded and analyzed. The results were presented as the mean (SD). The treatment groups were compared by an ANOVA using GraphPad Prism software (version 7.0).

Statistical Analysis

Statistical analysis was performed using graphing and statistical software (GraphPad Prism software, version 7.0; GraphPad, San Diego, CA, USA). The data are expressed as the mean (SD). Differences between two or more means were determined using unpaired t-test and 1-way ANOVA with Dunnett's post-test. Statistical significance was indicated in

Downloaded from hwmaint.iovs.org on 04/25/2024

Table. Real-Time PCR Was Performed Using Primers Specific for PLK1, CCNB1, CDK1, UBE2C, and CENPA

Gene	Forwards (5′-3′)	Reverse (5′-3′)	Product
PLK1	CATGTATACCTTGTTAGTGGGCAA	AGTAAAGAACTCGTCATTAAGCAGC	199bp
CCNB1	AATAAGGCGAAGATCAACATGGC	TTTGTTACCAATGTCCCCAAGAG	111bp
CDK1	GGATGTGCTTATGCAGGATTCC	CATGTACTGACCAGGAGGGATAG	100bp
UBE2C	GACCTGAGGTATAAGCTCTCGC	CAGGGCAGACCACTTTTCCTT	150bp
CENPA	GCCCTATTGGCCCTACAAGA	ACAGCAAAGTCCAGACAGCA	276bp
GAPDH	GGAGCGAGATCCCTCCAAAAT	GGCTGTTGTCATACTTCTCATGG	197bp

the following way: $^{*}P < 0.05$, $^{**}P < 0.01$, $^{***}P < 0.001$, and $^{****}P < 0.0001$.

Results

Xanthatin Selectively Inhibited Retinoblastoma

To identify specific inhibitors of retinoblastoma from Chinese herbal medicine, we performed differential cytotoxic drug screening on a panel of 89 natural products with 4 cancer cell lines, two retinoblastoma cell lines, Y79 and WERI-Rb1, and 2 UM cell lines, OMM2.3 and MEL290. This panel of 89 in-house compound libraries is composed of single components purified from Chinese herbal medicine (Fig. 1a). UM was used as the control cell line because it is the most common primary intraocular tumor among adults that is anatomically similar to retinoblastoma. Xanthatin was the top hit with a significantly higher inhibitory effect on retinoblastoma than other screened compounds. In retinoblastoma, the normalized cell viability of xanthatin was 27% (Y79) and 9% (WERI-Rb1; see Figs. 1b, c, Supplementary Table S1). In UM, the normalized cell viability of xanthatin was 39% (OMM2.3) and 46% (MEL290; see Figs. 1d, e, Supplementary Table S1). Thus, compared with UM, xanthatin preferentially inhibited the proliferation of retinoblastoma cells (see Fig. 1f).

We further evaluated the pharmacological efficacy of xanthatin by determining the IC_{50} values of the compound. Xanthatin effectively inhibited the proliferation of Y79 and WERI-Rb1 cells with IC_{50} values of 0.692 µM and 0.393 µM, respectively (Figs. 2c, d). The IC_{50} values of xanthatin for OMM2.3 and MEL290 cells were 2.811 µM and 2.289 µM, respectively (see Figs. 2e, f). The comparison of the IC_{50} values between retinoblastoma and UM clearly indicated that xanthatin selectively suppressed retinoblastoma growth in vitro (see Figs. 2g, h).

Xanthatin Inhibited the Proliferation of Retinoblastoma In Vivo

Xanthatin is an active ingredient isolated from TCM (see Fig. 2a) with reported antifungal and insecticidal activities and is used in the treatment of rhinitis, rheumatism, eczema, cancer, ulcer, and malaria.[23] To evaluate the pharmacological efficacy of xanthatin in vivo, we established a zebrafish xenograft model of retinoblastoma (Fig. 3a). The optical transparency of zebrafish combined with mCherry dye could help to detect tumor development within 1 week, and this model provided a unique possibility for high-resolution, noninvasive real-time imaging of fluorescently labeled cancer cells. In addition, when zebrafish embryos are immersed in water containing drugs, zebrafish can absorb small molecules directly from the water without requiring intravenous injection or other drug delivery methods.[24] We first determined the safe dose of xanthatin that had minimal impact on animal survival. The data indicated that the maximal safe dose of xanthatin in zebrafish was 5 µM (see Fig. 2b).

The 1-dpi (day post injection) embryos were treated with 5 µM xanthatin. At 6 dpi, the fluorescence intensity, which indicated a therapeutic effect, was recorded. The average fluorescence intensity was 99% ($n = 10$) in the control group and 19% ($n = 10$) in the drug treatment group, which showed that xanthatin significantly inhibited the growth of retinoblastoma cells in vivo by statistical analysis (see Fig. 3b).

Xanthatin Arrested the Cell Cycle and Induced Apoptosis in Retinoblastoma Cells

To elucidate the mechanism by which xanthatin inhibits the growth of retinoblastoma cells, we used flow cytometry to analyze the distribution of the cell cycle and apoptosis. The number of apoptotic cells increased in a dose-dependent manner in the xanthatin-treated group compared to the control group. Early apoptosis was predominant (annexin V+/PI-; Fig. 4a). The retinoblastoma protein (pRB) is a key governor of G1 progression. The loss of pRB function leads to uncontrolled cell division, recurrent genomic changes, and tumorigenesis.[25,26] As the concentration of xanthatin (0, 0.5, 1, and 2 µM) increased, the percentage of cells in the G2/M phase gradually increased, whereas the number of cells in the G1 phase gradually decreased (see Fig. 4b). The arrest of Y79 cells in the G2/M phase might be one of the underlying mechanisms by which xanthatin targets retinoblastoma. Taken together, xanthatin effectively arrested the cell cycle of retinoblastoma cells, induced early cellular apoptosis, and inhibited tumor growth.

Xanthatin Targeted the PLK1-Mediated G2/M Cell Cycle Pathway

Xanthatin has been reported to play a role in tumor suppression by inhibiting the STAT3-JAK2 signaling pathway in hepatocellular carcinoma and breast cancer.[27] Intriguingly, Western blot analysis showed that STAT3-JAK2 signaling was not affected in Y79 and WERI-Rb1 cells treated with xanthatin (Supplementary Fig. S1). The data suggested that xanthatin apparently did not exert its antitumor effect through the STAT3-JAK2 pathway in retinoblastoma cells.

To elucidate the potential mechanism of xanthatin in the treatment of retinoblastoma, we used comparative pharmacogenomic analysis to search for molecular evidence. By comparing the transcriptomes of Y79 and WERI-Rb1 cells treated with control or 1 µM xanthatin for 24 hours, we found that 70 genes were downregulated (Fig. 5a).

Investigative Ophthalmology & Visual Science

Downloaded from hwmaint.iovs.org on 04/25/2024

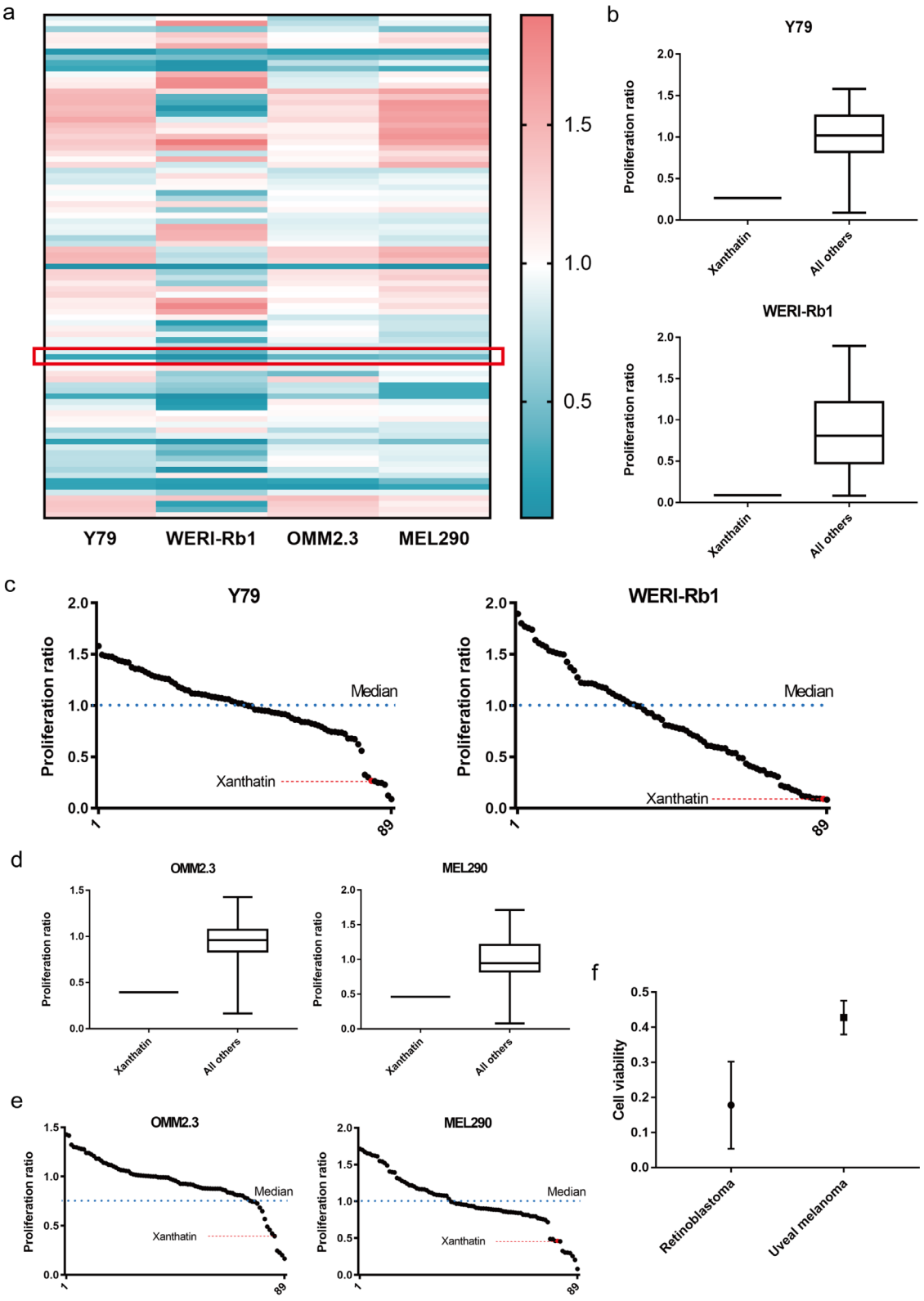

Figure 1. Identification of xanthatin. (**a**) Heatmap of drug sensitivity data. (**b**) Comparison of the cell viability after treatment of retinoblastoma with xanthatin versus all other screened compounds. (**c**) Plot of the cell viability of retinoblastoma after treatment with all 89 screened compounds. (**d**) Comparison of the cell viability of UM after treatment with xanthatin versus all other screened compounds. (**e**) Plot of the cell viability of UM after treatment with all 89 screened compounds. (**f**) Comparison of mean cell viability between the retinoblastoma and UM cell lines.

Investigative Ophthalmology & Visual Science

Downloaded from hwmaint.iovs.org on 04/25/2024

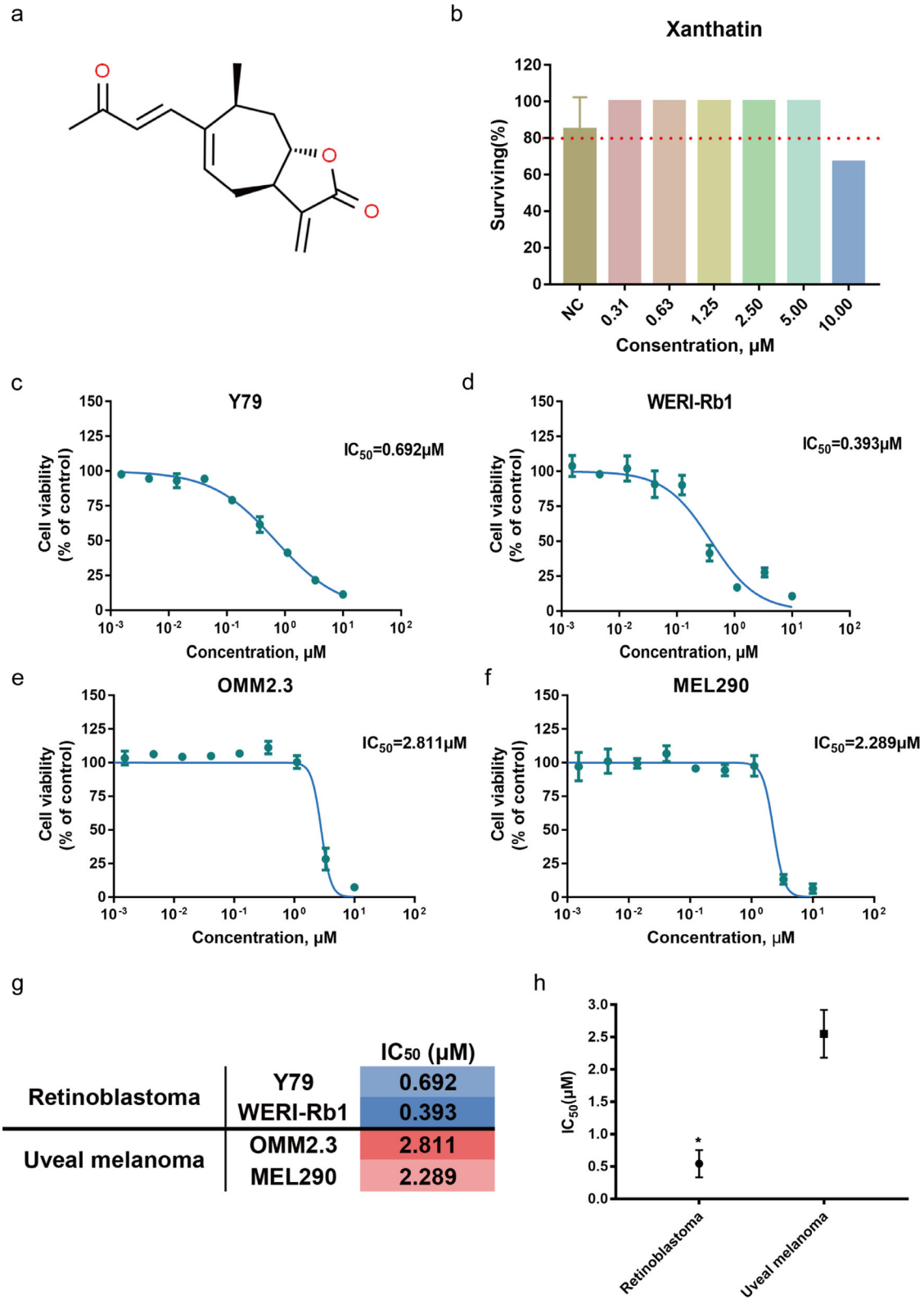

Figure 2. Antiproliferative effect of xanthatin on retinoblastoma. (**a**) Chemical structure of xanthatin ($C_{15}H_{18}O_3$; average mass: 246.302 Da). (**b**) Survival ratio of embryos after treatments with compounds at different concentrations. Uninjected 3-dpf embryos were placed in 24-well plates exposed to various concentrations of xanthatin. The survival of the embryos was examined until 8 dpf, $n = 12$; error bars show the standard error of the mean. (**c, d, e, f**) IC_{50} of xanthatin in two retinoblastoma and two UM cell lines. (**g**) Mean half maximal inhibitory (IC_{50} in [μM]) concentrations of xanthatin in the retinoblastoma and UM cell lines. (**h**) Comparison of the mean IC_{50} values between the retinoblastoma and UM lines. The *P* values are from unpaired *t* test, $^*P < 0.05$.

Investigative Ophthalmology & Visual Science

Downloaded from hwmaint.iovs.org on 04/25/2024

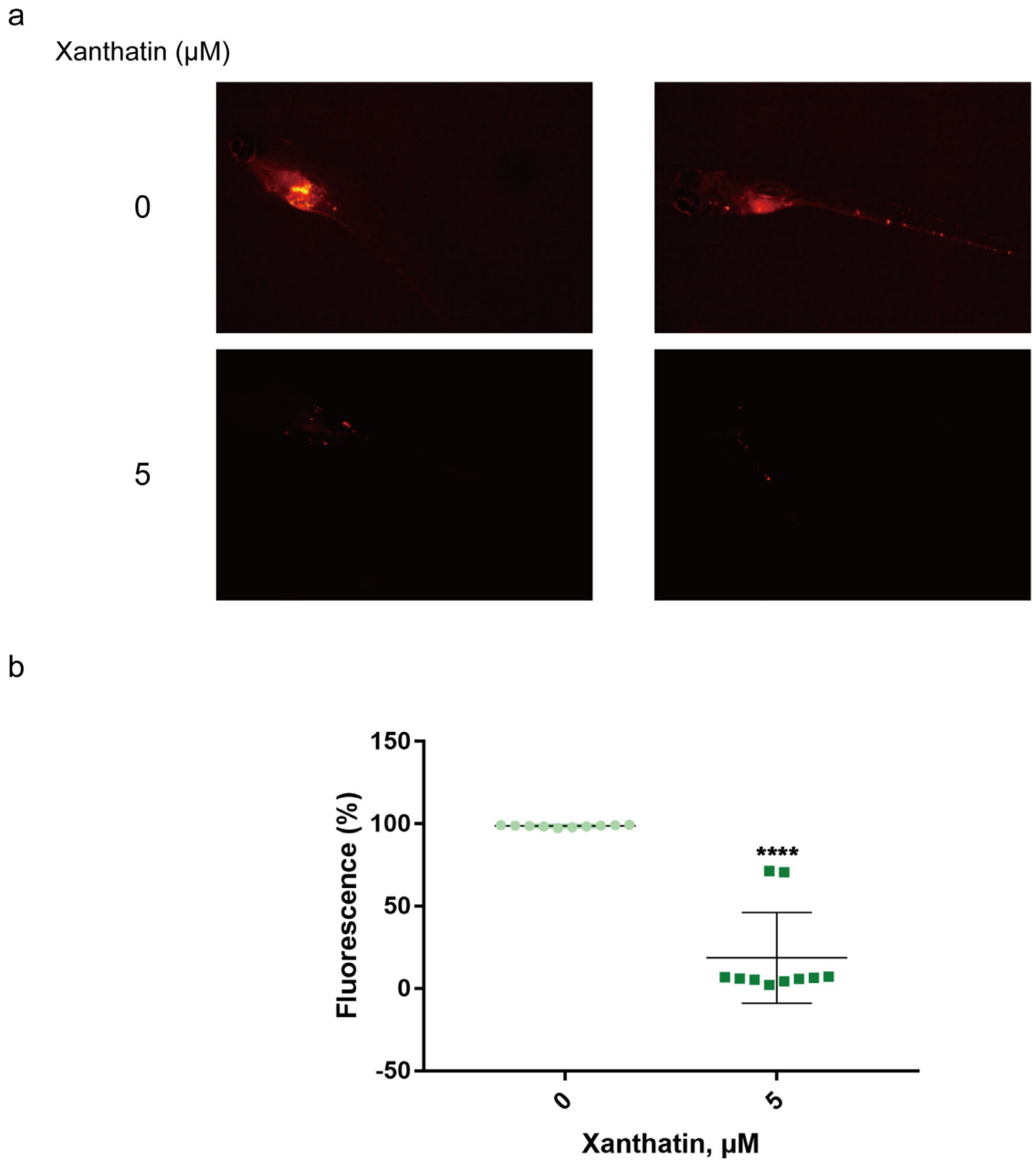

Figure 3. Xanthatin inhibited retinoblastoma growth in vivo. (**a**) TG(*flk:eGFP*) embryos (2 dpf) injected with Y79 cells with red fluorescence for easy observation. Zebrafish was treated with xanthatin (0 and 5 μM), $n = 10$. Six days after treatment, image capture, processing, and adjustment were performed. Scale bars, 200 μm for magnification images. (**b**) Statistical analysis showed that the fluorescence of the 5 μM xanthatin group was lower than that of the 0 μM xanthatin group. The *P* values are from unpaired *t* test, ****$P < 0.0001$.

Next, we aimed to verify the results of the pharmacogenomic profile of the DEGs (differentially expressed genes) in these samples, which were processed in the same way as sequencing samples. We found that the expression of polo-like kinase 1 (PLK1) was steadily downregulated (see Figs. 5b, c) after treatment with xanthatin, whereas the expression of other candidates could not be confirmed. Therefore, we hypothesized that PLK1 was the primary target of xanthatin in retinoblastoma cells.

We then examined whether the expression of other genes in the PLK1-mediated G2/M cell cycle pathway (PLK1, CCNB1, CDK1, UBE2C, and CENPA) was changed after xanthatin treatment. As expected, we found that the mRNA and protein levels of the above genes decreased in a concentration-dependent manner (see Figs. 5d, e). These results indicated that xanthatin inhibited cell proliferation through the PLK1-mediated G2/M cell cycle pathway in retinoblastoma (Fig. 6f).

Suppression of PLK1 Inhibited Retinoblastoma Progression In Vitro

PLK1 plays important roles throughout the M phase during cell cycle. To clarify the role of PLK1 in retinoblastoma, we collected tumor tissues from three patients, as well as the

Investigative Ophthalmology & Visual Science

Downloaded from hwmaint.iovs.org on 04/25/2024

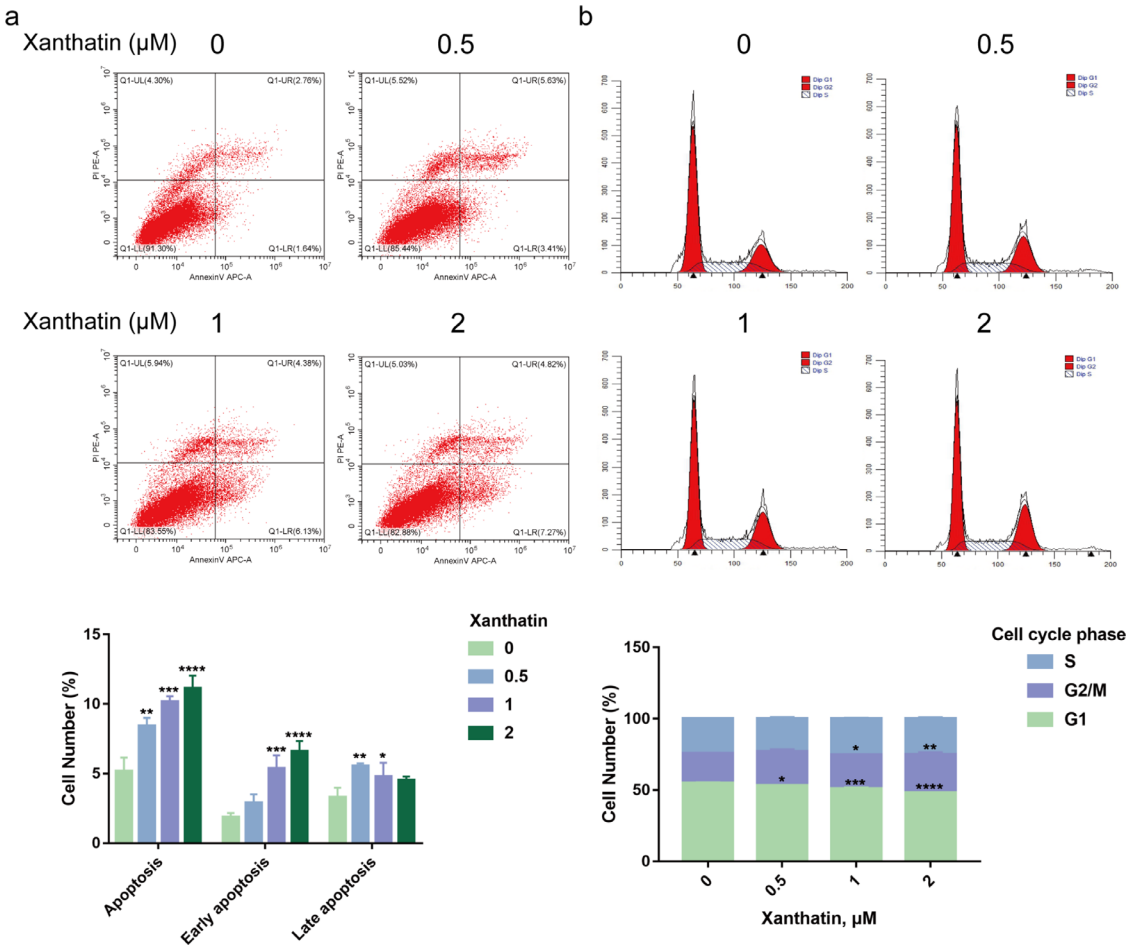

Figure 4. Xanthatin induced apoptosis and cell cycle arrest in Y79 cells. (**a**) The apoptosis of retinoblastoma cells was detected using FITC-AV/PI staining after treatment with xanthatin (0, 0.5, 1, and 2 μM) for 24 hours. (**b**) The cell cycle of retinoblastoma cells treated with xanthatin (0, 0.5, 1, and 2 μM) for 24 hours was detected using flow cytometry. The distribution of cells in the G1, G2/M, and S phases. The *P* values are from unpaired *t* test, **P* < 0.05, ***P* < 0.01, ****P* < 0.001, and *****P* < 0.0001.

paired normal tissue (GEO, https://www.ncbi.nlm.nih.gov/geo/, GEO accession number: GSE111168). Bioinformatics analysis showed that the level of PLK1 was higher in tumor tissues than that in normal tissues (see Fig. 6a). We next examined the expression of PLK1 in retinoblastoma cell lines. As expected, compared with the control cell ARPE-19, PLK1 was highly expressed in retinoblastoma cells (see Fig. 6b). The tumor characteristics upon PLK1 knockdown was further investigated. First, the expression level of PLK1 was knockdown by using three siRNAs and the efficiency was confirmed by Western blot (see Fig. 6c). Next, we estimated the role of PLK1 in Y79 cells. In CCK8 assay, tumor cell growth was significantly decreased in two siPLK1 Y79 cells, whereas the control cells retained a higher cell viability (see Fig. 6d). In addition, apoptosis was evaluated using flow cytometry by staining cells with APC-Annexin V and PI. Knockdown of PLK1 increased apoptosis in Y79 cells (see Fig. 6e). These data indicated that PLK1 played an important regulatory role in cell death through apoptosis.

Discussion

Xanthatin is an anti-inflammatory compound derived from the plant Xanthium L.[28] Xanthatin has been used as a Chinese herbal medicine in the treatment of rhinitis for thousands of years in China. Xanthatin has been shown to effectively inhibit the proliferation of many cancer cells, such as melanoma cells, lung cancer cells, and hepatocellular carcinoma cells.[29–35] By using differential cytotoxic drug screening, we discovered that xanthatin arrested cell cycle progression and induced apoptosis in retinoblastoma cells by suppressing the PLK1-mediated G2/M cell cycle pathway. Remarkably, xanthatin is an outstanding sesquiterpene lactone compound with impressive antitumor activity that exhibits little toxicity in zebrafish. Therefore, xanthatin might be used as an effective antitumor compound to expand its clinical indications.

Natural products are an abundant source of drug candidates for cancer treatment.[15] Identification of individual components with favorable pharmacological profiles may offer beneficial outcomes. Here, we used an unbiased drug screening system, which provided an opportunity to explore the biological behavior of cancer cells at the cellular level and to identify a number of clinical stage drugs with anticancer properties. Our compound library could identify new bioactivities of previously approved drugs, which is known as drug repurposing. This new use of old drugs could provide us with comprehensive insight into dynamic

Downloaded from hwmaint.iovs.org on 04/25/2024

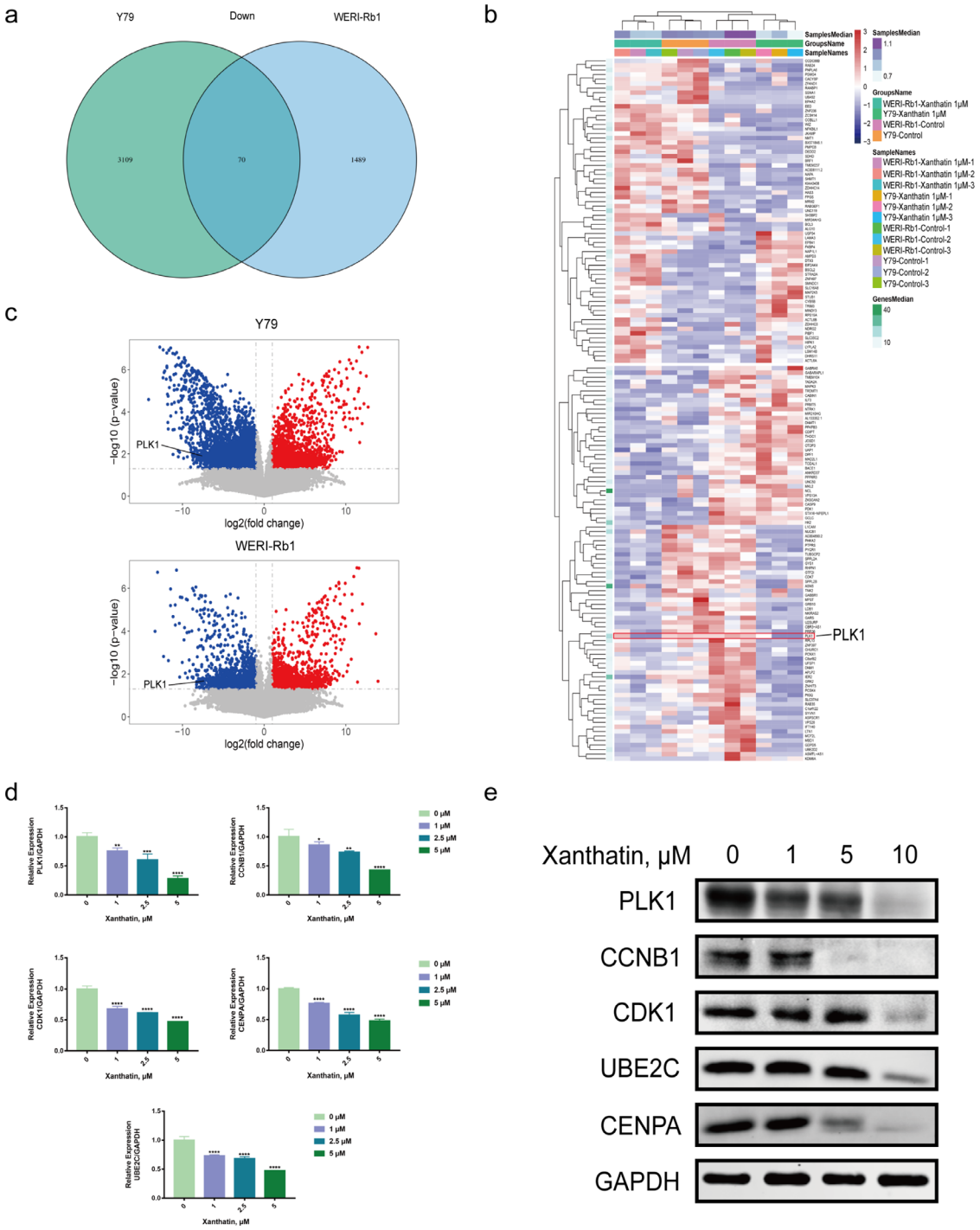

Figure 5. Xanthatin targeted PLK in Y79 cells. (**a**) Seventy downregulated genes were differentially expressed in two retinoblastoma cell lines (fold change ≥ 1.5, FDR < 0.05). (**b**) Heatmap of total 238 DEGs in two cell lines. (**c**) Volcano plots of DEGs. The X-axis represents log fold changes. The Y-axis represents log *P* values. The blue points denote the significantly downregulated genes, and the red points denote the significantly upregulated genes. (**d, e**) The efficiency of the PLK1-mediated G2/M cell cycle pathway in Y79 cells was verified by real-time PCR **d** and Western blot **e**. Error bars represent the SD of three replicates. The *P* values were from 1-way ANOVA, $^{*}P < 0.05$, $^{**}P < 0.01$, $^{***}P < 0.001$, and $^{****}P < 0.0001$.

pharmacogenomics interactions across multiple cancer types. In addition, the advantages of this approach include cost-effectiveness, parallel data generation, and rapid drug development.[36,37] We first used this compound screening system for repurposing natural products as drug candidates on retinoblastoma cell lines. The results show that this method is useful for the discovery of new drugs against retinoblastoma.

We also used the zebrafish system to assess drug efficacy and toxicity in vivo to determine the safety and effectiveness of natural products. Zebrafish is an ideal animal model system.[38] The Zebrafish xenograft model has already been

Investigative Ophthalmology & Visual Science

Downloaded from hwmaint.iovs.org on 04/25/2024

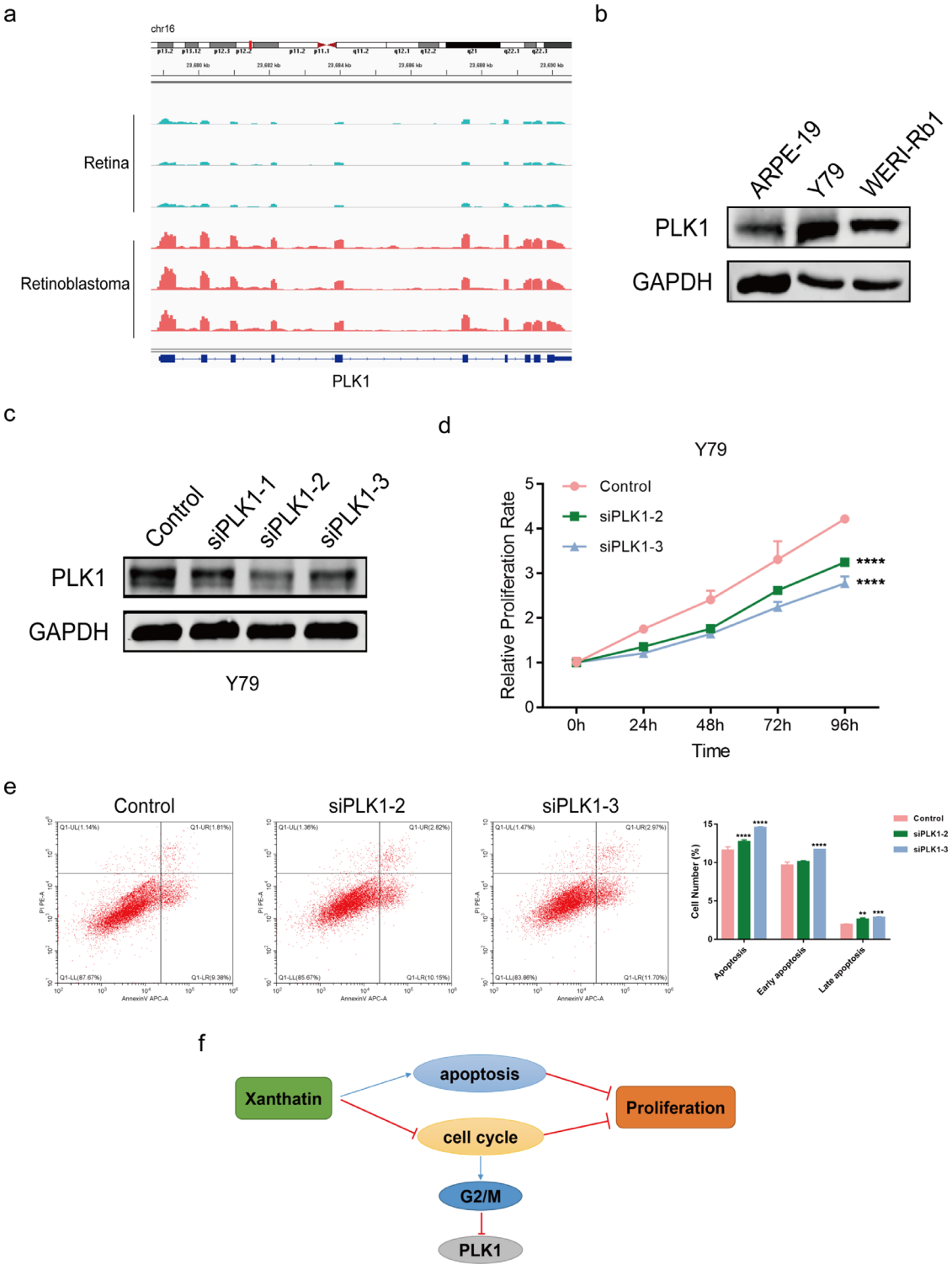

Figure 6. PLK1 contributed to tumor progression. (**a**) RNA-sequence analysis was performed to evaluate the transcriptome of three retinoblastoma samples and normal retina samples. (**b**) The expression level of PLK1 in the retinoblastoma cells was verified by Western blot. (**c**) Efficiency of PLK1 knockdown in Y79 cells by siRNAs was verified by Western blot. (**d**) CCK8 assay showing tumor cell growth after PLK1 knockdown. Cell growth was restrained in PLK1 KD Y79 cells. The absorbance values were detected at 0, 24, 48, 72, and 96 hours, and the control was arbitrarily set at 100% on 0 hour. $^{****}P < 0.0001$. (**e**) siPLK1 Y79 cells were more prone to apoptosis. The percentage of apoptotic cells was analyzed by flow cytometry. Error bars represent the SD of three replicates. The *P* values were from two-way ANOVA, $^{**}P < 0.01$, $^{***}P < 0.001$, and $^{****}P < 0.0001$. (**f**) Schematic model of xanthatin inhibiting retinoblastoma cell growth via the PLK1-mediated G2/M cell cycle pathway.

Downloaded from hwmaint.iovs.org on 04/25/2024

widely accepted for investigating cancer and cancer therapeutics. It is also used in ocular cancer studies.[18,39–43] The general advantages of this model included relatively low cost, transparency, and easy manipulation of the embryo. In recent years, high-throughput technology has improved the role of zebrafish embryos in screening for chemical drugs.[44,45] Because zebrafish can autonomously absorb small molecular weight compounds from water, the operation was simple and effective.[46,47] Our results showed that zebrafish could be an important model for the discovery of new drugs and new therapeutic strategies.

We found that xanthatin exerted its antiproliferative effects by arresting retinoblastoma cells in the G2/M phase. It is well known that cell growth is controlled by the cell cycle process, which is highly regulated.[48] Unlike normal cells, which rely on the G1 checkpoint to prevent DNA damage, cancer cells rely more on the G2 checkpoint to repair DNA damage.[49] Therefore, the cell cycle G2 checkpoint has been proposed to be a specific target for cancer treatment.[50–52] Further experimental data revealed that xanthatin targeted PLK1 and its related signaling pathways. *PLK1* plays important roles throughout the M phase of the cell cycle, including the regulation of centrosome maturation and spindle assembly, the removal of cohesins from chromosome arms, the inactivation of anaphase-promoting complex/cyclosome (APC/C) inhibitors, and the regulation of mitotic exit and cytokinesis.[53] Previous studies have shown that PLK1 is overexpressed in a variety of human tumors and is a potential biomarker for cancer prognosis. It is involved in the development of cancer and has potential as a therapeutic target.[54,55] Furthermore, role of PLK1 has also been reported in retinoblastoma. The expression level of PLK1 was related to histopathological high-risk factors and poor tumor differentiation.[56] Combined hyperthermia (HT) therapy with PLK1 knockdown could enhance the sensitivity of retinoblastoma cells toward HT-associated apoptosis.[57] This suggested that the inhibition of PLK was effective in inducing death of retinoblastoma cells.

It has been reported that PLK1 is a target of the retinoblastoma tumor suppressor (*RB*) pathway in cancers. The activation of *RB* and the related pocket proteins *p107/p130* results in the repression of PLK1 promoter activity. Conversely, the loss of *RB* released the suppression of *PLK1*.[58,59] Importantly, 95% of patients with retinoblastoma have loss-of-function *RB1* mutations.[60,61] Thus, the specificity of *RB1* genetic status mediated the sensitivity of retinoblastoma to PLK inhibitors.

In conclusion, we discovered a natural compound, xanthatin, that could effectively inhibit the proliferation of retinoblastoma. Mechanistically, xanthatin inhibited the cell cycle and induced the apoptosis of human retinoblastoma cells by targeting the PLK1-mediated G2/M cell cycle pathway. We also proposed a new method to identify anti-retinoblastoma drugs and evaluate their efficacy in vivo with a zebrafish model.

Acknowledgments

Supported and funded by 2021 Zhangjiang Science and Technology Project (RC20210152), the National Natural Science Foundation of China (grants 81872339, 82073889), the National Facility for Translational Medicine (Shanghai) (TMSZ-2020-206), the Science and Technology Commission of Shanghai (20DZ2270800), the Shanghai Science and Technology Development Funds (19QA1405100), Youth Medical Talents-Specialist Program and Shanghai Youth Top-notch Talent Support Program, the Shanghai Ninth People's Hospital training program (jyyq09201713, the Young doctors' innovation team (QC201805) and Shanghai "Rising Stars of Medical Talent" Youth Development Program.

Disclosure: **J. Yang,** None; **Y. Li,** None; **C. Zong,** None; **Q. Zhang,** None; **S. Ge,** None; **L. Ma,** None; **J. Fan,** None; **J. Zhang,** None; **R. Jia,** None

References

1. Kivelä T. The epidemiological challenge of the most frequent eye cancer: retinoblastoma, an issue of birth and death. *Br J Ophthalmol*. 2009;93:1129–1131.
2. Parkin DM, Stiller CA, Draper GJ, Bieber CA. The international incidence of childhood cancer. *Intl J Cancer*. 1988;42:511–520.
3. Global Retinoblastoma Study G,Fabian ID, Abdallah E, et al. Global Retinoblastoma Presentation and Analysis by National Income Level. *JAMA Oncol*. 2020;6:685–695.
4. Tomar AS, Finger PT, Gallie B, et al. Global Retinoblastoma Treatment Outcomes: Association with National Income Level. *Ophthalmology*. 2021;128:740–753.
5. Fabian ID, Stacey AW, Foster A, et al. Travel burden and clinical presentation of retinoblastoma: analysis of 1024 patients from 43 African countries and 518 patients from 40 European countries. *Br J Ophthalmol*. 2021;105:1435–1443.
6. Tomar AS, Finger PT, Gallie B, et al. A Multicenter, International Collaborative Study for American Joint Committee on Cancer Staging of Retinoblastoma: Part II: Treatment Success and Globe Salvage. *Ophthalmology*. 2020;127:1733–1746.
7. Kaliki S, Shields CL. Retinoblastoma: achieving new standards with methods of chemotherapy. *Indian J Ophthalmol*. 2015;63:103–109.
8. Shields CL, Fulco EM, Arias JD, et al. Retinoblastoma frontiers with intravenous, intra-arterial, periocular, and intravitreal chemotherapy. *Eye (Lond)*. 2013;27:253–264.
9. Shields CL, Bas Z, Tadepalli S, et al. Long-term (20-year) real-world outcomes of intravenous chemotherapy (chemoreduction) for retinoblastoma in 964 eyes of 554 patients at a single centre. *Br J Ophthalmol*. 2020;104:1548–1555.
10. Manjandavida FP, Stathopoulos C, Zhang J, Honavar SG, Shields CL. Intra-arterial chemotherapy in retinoblastoma - A paradigm change. *Indian J Ophthalmol*. 2019;67:740–754.
11. Dalvin LA, Ancona-Lezama D, Lucio-Alvarez JA, Masoomian B, Jabbour P, Shields CL. Ophthalmic Vascular Events after Primary Unilateral Intra-arterial Chemotherapy for Retinoblastoma in Early and Recent Eras. *Ophthalmology*. 2018;125:1803–1811.
12. Xue K, Ren H, Meng F, Zhang R, Qian J. Ocular toxicity of intravitreal melphalan for retinoblastoma in Chinese patients. *BMC Ophthalmol*. 2019;19:61.
13. Munier FL, Beck-Popovic M, Chantada GL, et al. Conservative management of retinoblastoma: Challenging orthodoxy without compromising the state of metastatic grace. "Alive, with good vision and no comorbidity". *Prog Retinal Eye Res*. 2019;73:100764.
14. Guo W, Tan HY, Chen F, Wang N, Feng Y. Targeting Cancer Metabolism to Resensitize Chemotherapy: Potential Development of Cancer Chemosensitizers from Traditional Chinese Medicines. *Cancers (Basel)*. 2020;12:404.
15. Hao P, Jiang F, Cheng J, Ma L, Zhang Y, Zhao Y. Traditional Chinese Medicine for Cardiovascular Disease: Evidence and Potential Mechanisms. *J Am Coll Cardiol*. 2017;69:2952–2966.

Downloaded from hwmaint.iovs.org on 04/25/2024

16. Zhao C, Li S, Zhang J, et al. Current state and future perspective of cardiovascular medicines derived from natural products. *Pharmacol Ther*. 2020;216:107698.
17. Yao CL, Zhang JQ, Li JY, Wei WL, Wu SF, Guo DA. Traditional Chinese medicine (TCM) as a source of new anticancer drugs. *Nat Prod Rep*. 2021;38:1618–1633.
18. van der Ent W, Burrello C, Teunisse AF, et al. Modeling of human uveal melanoma in zebrafish xenograft embryos. *Invest Ophthalmol Vis Sci*. 2014;55:6612–6622.
19. Wojciechowska S, van Rooijen E, Ceol C, Patton EE, White RM. Generation and analysis of zebrafish melanoma models. *Methods Cell Biol*. 2016;134:531–549.
20. Patel RK, Jain M. NGS QC Toolkit: a toolkit for quality control of next generation sequencing data. *PLoS One*. 2012;7:e30619.
21. Pertea M, Pertea GM, Antonescu CM, Chang TC, Mendell JT, Salzberg SL. StringTie enables improved reconstruction of a transcriptome from RNA-seq reads. *Nat Biotechnol*. 2015;33:290–295.
22. Anders S, Huber W. Differential expression analysis for sequence count data. *Genome Biol*. 2010;11:R106.
23. Nibret E, Youns M, Krauth-Siegel RL, Wink M. Biological activities of xanthatin from Xanthium strumarium leaves. *Phytother Res*. 2011;25:1883–1890.
24. Zon L, Peterson R. In vivo drug discovery in the zebrafish. *Nat Rev Drug Discov*. 2005;4:35–44.
25. Classon M, Harlow E. The retinoblastoma tumour suppressor in development and cancer. *Nat Rev Cancer*. 2002;2:910–917.
26. Weinberg RA. *The biology of cancer*. Second edition. New York, NY: W. W. Norton & Company; 2014.
27. Liu M, Xiao C, Sun M, Tan M, Hu L, Yu Q. Xanthatin inhibits STAT3 and NF-κB signalling by covalently binding to JAK and IKK kinases. *J Cell Molec Med*. 2019;23:4301–4312.
28. Ju A, Cho YC, Cho S. Methanol extracts of Xanthium sibiricum roots inhibit inflammatory responses via the inhibition of nuclear factor-kappaB (NF-kappaB) and signal transducer and activator of transcription 3 (STAT3) in murine macrophages. *J Ethnopharmacol*. 2015;174:74–81.
29. Tao L, Cao Y, Wei Z, et al. Xanthatin triggers Chk1-mediated DNA damage response and destabilizes Cdc25C via lysosomal degradation in lung cancer cells. *Toxicol Applied Pharmacol*. 2017;337:85–94.
30. Li WD, Wu Y, Zhang L, et al. Characterization of xanthatin: Anticancer properties and mechanisms of inhibited murine melanoma in vitro and in vivo. *Phytomedicine*. 2013;20:865–873.
31. Ma YY, Di ZM, Cao Q, et al. Xanthatin induces glioma cell apoptosis and inhibits tumor growth via activating endoplasmic reticulum stress-dependent CHOP pathway. *Acta Pharmacol Sin*. 2020;41:404–414.
32. Tao L, Sheng X, Zhang L, et al. Xanthatin anti-tumor cytotoxicity is mediated via glycogen synthase kinase-3β and β-catenin. *Biochem Pharmacol*. 2016;115:18–27.
33. Zhang L, Ruan J, Yan L, et al. Xanthatin induces cell cycle arrest at G2/M checkpoint and apoptosis via disrupting NF-kappaB pathway in A549 non-small-cell lung cancer cells. *Molecules*. 2012;17:3736–3750.
34. Shi T-l, Zhang L, Cheng Q-y, et al. Xanthatin induces apoptosis by activating endoplasmic reticulum stress in hepatoma cells. *Eur J Pharmacol*. 2019;843:1–11.
35. Piloto-Ferrer J, Sanchez-Lamar A, Francisco M, et al. Xanthium strumarium s xanthatins induces mitotic arrest and apoptosis in CT26WT colon carcinoma cells. *Phytomedicine*. 2019;57:236–244.
36. Wermuth C. Selective optimization of side activities: another way for drug discovery. *J Medicinal Chem*. 2004;47:1303–1314.
37. Nosengo N. Can you teach old drugs new tricks? *Nature*. 2016;534:314–316.
38. Horzmann KA, Freeman JL. Making Waves: New Developments in Toxicology With the Zebrafish. *Toxicol Sci*. 2018;163:5–12.
39. Chen X, Wang J, Cao Z, et al. Invasiveness and metastasis of retinoblastoma in an orthotopic zebrafish tumor model. *Sci Rep*. 2015;5:10351.
40. Ding Y, Yu J, Chen X, et al. Dose-Dependent Carbon-Dot-Induced ROS Promote Uveal Melanoma Cell Tumorigenicity via Activation of mTOR Signaling and Glutamine Metabolism. *Advanced Science (Weinheim, Baden-Wurttemberg, Germany)*. 2021;8:2002404.
41. Chen Q, Ramu V, Aydar Y, et al. TLD1433 Photosensitizer Inhibits Conjunctival Melanoma Cells in Zebrafish Ectopic and Orthotopic Tumour Models. *Cancers (Basel)*. 2020;12:587.
42. Gyda M, Wolman M, Lorent K, Granato M. The tumor suppressor gene retinoblastoma-1 is required for retinotectal development and visual function in zebrafish. *PLoS Genet*. 2012;8:e1003106.
43. Jo DH, Son D, Na Y, et al. Orthotopic transplantation of retinoblastoma cells into vitreous cavity of zebrafish for screening of anticancer drugs. *Molec Cancer*. 2013;12:71.
44. Idilli AI, Precazzini F, Mione MC, Anelli V. Zebrafish in Translational Cancer Research: Insight into Leukemia, Melanoma, Glioma and Endocrine Tumor Biology. *Genes (Basel)*. 2017;8:236.
45. Facciol A, Tsang B, Gerlai R. Alcohol exposure during embryonic development: An opportunity to conduct systematic developmental time course analyses in zebrafish. *Neurosci Biobehav Rev*. 2019;98:185–193.
46. Liu S, Leach SD. Zebrafish models for cancer. *Annu Rev Pathol*. 2011;6:71–93.
47. Jung DW, Oh ES, Park SH, et al. A novel zebrafish human tumor xenograft model validated for anti-cancer drug screening. *Mol Biosyst*. 2012;8:1930–1939.
48. Sancar A, Lindsey-Boltz LA, Unsal-Kacmaz K, Linn S. Molecular mechanisms of mammalian DNA repair and the DNA damage checkpoints. *Annu Rev Biochem*. 2004;73:39–85.
49. Löbrich M, Jeggo P. The impact of a negligent G2/M checkpoint on genomic instability and cancer induction. *Nat Rev Cancer*. 2007;7:861–869.
50. Bassermann F, Pagano M. Dissecting the role of ubiquitylation in the DNA damage response checkpoint in G2. *Cell Death Differ*. 2010;17:78–85.
51. Wang Y, Ji P, Liu J, Broaddus RR, Xue F, Zhang W. Centrosome-associated regulators of the G(2)/M checkpoint as targets for cancer therapy. *Molec Cancer*. 2009;8:8.
52. Shapiro GI, Harper JW. Anticancer drug targets: cell cycle and checkpoint control. *J Clin Invest*. 1999;104:1645–1653.
53. Mandal R, Strebhardt K. Plk1: unexpected roles in DNA replication. *Cell Res*. 2013;23:1251–1253.
54. Strebhardt K, Ullrich A. Targeting polo-like kinase 1 for cancer therapy. *Nat Rev Cancer*. 2006;6:321–330.
55. Strebhardt K. Multifaceted polo-like kinases: drug targets and antitargets for cancer therapy. *Nat Rev Drug Discov*. 2010;9:643–660.
56. Singh L, Pushker N, Sen S, Singh MK, Chauhan FA, Kashyap S. Prognostic significance of polo-like kinases in retinoblastoma: correlation with patient outcome, clinical and histopathological parameters. *Clin Exp Ophthalmol*. 2015;43:550–557.
57. Yunoki T, Tabuchi Y, Hayashi A, Kondo T. Inhibition of polo-like kinase 1 promotes hyperthermia sensitivity via inactivation of heat shock transcription factor 1 in human retinoblastoma cells. *Invest Ophthalmol Vis Sci*. 2013;54:8353–8363.

Investigative Ophthalmology & Visual Science

Downloaded from hwmaint.iovs.org on 04/25/2024

58. Gunawardena RW, Siddiqui H, Solomon DA, et al. Hierarchical requirement of SWI/SNF in retinoblastoma tumor suppressor-mediated repression of Plk1. *J Biol Chem*. 2004;279:29278–29285.
59. Witkiewicz AK, Chung S, Brough R, et al. Targeting the Vulnerability of RB Tumor Suppressor Loss in Triple-Negative Breast Cancer. *Cell Reports*. 2018;22:1185–1199.
60. Cavenee WK, Dryja TP, Phillips RA, et al. Expression of recessive alleles by chromosomal mechanisms in retinoblastoma. *Nature*. 1983;305:779–784.
61. Friend SH, Bernards R, Rogelj S, et al. A human DNA segment with properties of the gene that predisposes to retinoblastoma and osteosarcoma. *Nature*. 1986;323:643–646.

Investigative Ophthalmology & Visual Science

Downloaded from hwmaint.iovs.org on 04/25/2024